MDPI

Article

Aircraft emissions, their plume-scale effects, and the nonlinear response of the climate-chemistry system

Kieran Tait [1,†,‡], Firstname Lastname [1,‡] and Firstname Lastname [2,*]

[1] University of Bristol; kt16229@bristol.ac.uk
[2] Affiliation 2; e-mail@e-mail.com
* Correspondence: e-mail@e-mail.com; Tel.: (optional; include country code; if there are multiple corresponding authors, add author initials) +xx-xxxx-xxx-xxxx (F.L.)
† Current address: Affiliation 3
‡ These authors contributed equally to this work.

Keywords: keyword 1; keyword 2; keyword 3 (List three to ten pertinent keywords specific to the article; yet reasonably common within the subject discipline.)

Citation: Tait, K.; Lastname, F.; Lastname, F. Aircraft emissions, their plume-scale effects, and the nonlinear response of the climate-chemistry system. *Aerospace* **2021**, *1*, 0. https://doi.org/

Received:
Accepted:
Published:

1. Introduction

Aircraft act as high-altitude emissions vectors, transporting a number of radiatively and chemically active substances across vast regions of the globe. These substances induce a net global warming effect that constitutes 3.5% of the global climate impact due to anthropogenic sources **??**. Two thirds of this impact result from aircraft non-CO2 emissions, which have a variable impact depending on when and where they are released. This means that avoiding flying in climate-sensitive regions of the atmosphere has the potential to reduce aviation's climate impact significantly **??**. Furthermore, the environmental conditions within the aircraft exhaust plume result in additional chemical and microphysical processing that is not accounted for in global chemistry models. In high-density airspace, such as along the North Atlantic Flight Corridor, aircraft often fly in close proximity, giving rise to the superposition of their plumes and the accumulation of emissions contained within them **??**. It has been shown in **??** that the overlap of four consecutive plumes can influence the nonlinear chemistry and microphysics significantly, leading to saturation effects that can potentially provide a net climate impact reduction.

2. Aircraft emissions

Aircraft propulsion systems provide the essential driving force component to enable powerful and efficient flight, however convention has dictated the use of hydrocarbons as the primary source of aviation fuels since the dawn of powered flight. In commercial aviation, responsible for 88% of global aviation fuel usage [1], it is commonplace to use a gas turbine propulsion system operating on kerosene-based jet fuel. Aviation's environmental impact stems from the emission and dispersion of chemically and radiatively active substances, that are generated during the jet fuel combustion process. The combustion of fuel and the generation of emissions is closely coupled with

the performance of aircraft, and the forces and dynamics experienced throughout flight. This section explores the coupling between aircraft performance and the generation of aviation-induced climate forcing species, before reviewing the emissions modelling techniques present in the current literature.

2.1. The need for propulsion

For an aircraft to achieve and maintain airborne status, it is required that the resistive force due to aerodynamic drag (D) and the gravitational force due to aircraft weight (W) are sufficiently overcome. The necessary driving force required to counteract drag and maintain forward speed is known as thrust (T). The forward speed induces airflow over the aircraft's cambered wings, thus rotating the flow downwards and generating lift (L) to counteract the aircraft weight. This constitutes the four fundamental forces of flight [2]. The combination of these forces in varying magnitudes determines the trajectory of an aircraft and its instantaneous velocity and acceleration.

The performance of an aircraft is highly dependent on the optimisation of the four forces, with structural configuration, material utilisation and payload affecting the aircraft's weight, balance and stability, and the aircraft geometry affecting aerodynamics and hence influencing the lift and drag forces acting upon it. The thrust force however, is generated by means of a propulsion system.

Gas turbine engines employ the following four point Brayton thermodynamic cycle (see figure 1): (1) the engine intakes oncoming air flow, (2) the air passes through a compressor to increase its total pressure, (3) the compressed air is mixed with fuel and ignited to cause a combustion reaction and (4) the high temperature, high pressure combustion products are passed through a turbine which extracts some energy from the flow to drive the compressor, before the airflow exits the engine at an accelerated rate, through the exhaust nozzle. The magnitude of thrust generated by the engine is dependent on the mass of air being accelerated, and the difference in velocity of the air mass through the propulsion system.

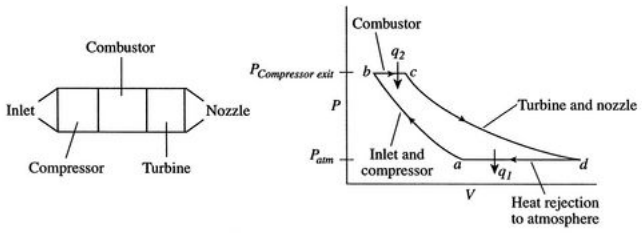

Figure 1. Brayton cycle [].

2.2. The jet fuel combustion process

The widespread usage of kerosene-based jet fuels stems from the need to satisfy strict power-to-weight and safety requirements demanded by commercial aircraft; this is because kerosene has an exceptionally high energy density and wide operating temperature range at a low financial cost, compared to alternative fuel types. The stoichiometric combustion of kerosene with air required to generate

thrust, does however generate a number of additional chemical species which are emitted into the aircraft wake. These aircraft emissions interact with the surrounding atmosphere, perturbing the natural balance of chemistry and contributing to air quality issues and anthropogenic climate change. The mass of emission produced per unit mass of fuel burnt is often referred to as the emission index (EI), measured in grams of emission per kilogram of fuel [g/kg].

The primary products of ideal jet fuel combustion are water vapour (H_2O), carbon dioxide (CO_2) and, due to fuel impurities, a relatively small amount of sulphur oxides (SO_x). Additionally, a number of secondary combustion products are generated in varying quantities, depending on their formation mechanisms and the nature of the combustion process. The most common of these products are oxides of nitrogen (NO_x = NO + NO_2), carbon monoxide (CO), unburnt hydrocarbons (HC), particulate matter (PM) and volatile organic compounds (VOCs) [3].

2.3. The generation of aircraft emissions

The generation of primary jet fuel combustion products, H_2O, CO_2 and SO_x, depend purely on the carbon-hydrogen-sulfur composition of the fuel. This means that for a constant fuel composition, these species have a constant EI throughout the entire range of operating conditions and therefore they are directly coupled to the amount of fuel burnt. The EIs of the secondary combustion products however, are variable depending on the type of aircraft engine, engine operating conditions, and the state of the surrounding atmosphere [4].

The entry of atmospheric nitrogen (N_2) into the high temperature combustion chamber leads to the formation and emission of nitrogen oxides (NO_x = NO + NO_2). The levels of NO_x emitted from aircraft engines increases with temperature and pressure in the primary combustion zone. Therefore, [illegible] the assumption of constant polytropic and combustion efficiencies, the emission index of NO_x ($EINO_x$) can be correlated with aircraft fuel flow [5].

As a result of inefficiencies in the combustion process, products such as carbon monoxide (CO), unburnt hydrocarbons (HC) are formed. The levels of CO and HC on the other hand, are direct products of incomplete combustion, and hence their concentrations are inversely proportional to combustion efficiency. Since combustion efficiency correlates with thrust for sea level static (SLS) conditions (see [5] figure 4.), and fuel flow correlates with thrust, this means that EICO and EIHC decrease with increasing fuel flow.

Trace levels of soot, particulate matter (PM) and volatile organic compounds (VOCs) are also generated, however often in relatively small amounts, and the mechanisms that lead to their production are complex and out of the scope of this review. See [4] for more details on this.

2.4. Aircraft emissions modelling

Accurate quantification of aircraft emissions requires the calculation of aircraft performance to estimate the total energy consumed, and hence, the total fuel burnt throughout the duration of a flight. With

knowledge of the fuel flow rates experienced throughout flight, flow rates of aircraft emission species can be deduced based on empirical engine performance datasets and emissions models.

2.4.1. Fuel burn estimation

Computational modelling of aircraft performance allows the simulation of aircraft trajectories and the quantification of forces experienced throughout flight, enabling the approximation of thrust and fuel flow across all phases of flight. Aircraft performance models that are prevalent in academia and industry, such as the BADA (Base of Aircraft DAta) method [6] and PIANO-X [7], emulate aircraft behaviour by coupling a database of aircraft-specific performance datasets to mathematical models to calculate useful flight characteristics, such as fuel flow and fuel burn, at discrete time steps during flight. This iterative approach accounts for the time-varying nature of aircraft properties like mass, speed and heading, thus leading to a more accurate analysis of performance and fuel burn estimation. Further to this, models such as the Aviation Environment Design Tool (AEDT) [8] exist, which carry out four-dimensional (4-D) physics-based simulations of aircraft trajectories at an exceptionally high spatial and temporal resolution, providing highly accurate predictions of fuel consumption and localised emissions impacts. Such tools do however come at the expense of high computational and financial cost, and often require proprietary data that is unavailable to the public domain.

2.4.2. Calculating aircraft emissions at reference conditions

As previously alluded to in section 2.3, the primary combustion products, CO_2, H_2O and SO_x have a direct relation to the amount of fuel burnt and hence a constant EI for a given fuel composition, whereas the secondary products largely depend on operational and atmospheric conditions. Emissions of NO_x, CO and HC can be correlated with fuel flow, meaning estimation of their emission indices requires knowledge of this relationship across the range of operating conditions experienced throughout flight. Empirical relationships have been determined using engine performance datasets, such as the ICAO engine emissions databank [9]. The ICAO engine emissions databank was developed for the purpose of engine certification and compliance with landing and take-off (LTO) cycle emissions standards, outlined in ICAO Annex 16 Vol. II [10]. Engine test data have been collected at SLS, International Standard Atmosphere (ISA) conditions, for four reference operating conditions (thrust settings) relevant to the LTO cycle: take-off (100% thrust), climb out (85%), approach (30%) and taxi in/out (7%). For every engine at each of the four LTO modes, a reference fuel flow and corresponding emission index has been derived, allowing emissions to be estimated for aircraft operating under any of the four modes, to a reasonable degree of accuracy.

Table 1: Example ICAO engine emissions data for Rolls Royce Trent 970-84 engine [9].

	Take-off	Climb out	Approach	Idle
Fuel flow [kg/s]	2.605	2.157	0.720	0.255
EI NO_x [g/kg]	38.29	29.42	12.09	5.44
EI CO [g/kg]	0.32	0.31	1.16	13.38
EI HC [g/kg]	0.02	0.12	0.08	0.04

2.4.3. Calculating aircraft emissions at non-reference conditions

In reality, aircraft spend the majority of flight outside of the LTO vicinity (above 3,000 ft), and the operating conditions and atmospheric conditions vary considerably. To enable the accurate analysis of aircraft emissions outside of reference conditions, a number of emissions modelling methods have been developed, which apply the necessary adjustments and interpolations to the LTO-limited engine performance datasets, to generate more realistic estimates of aircraft emissions across the whole flight profile. [11] describes a number of methods for calculating aircraft emissions throughout all modes of operation and compares their relative merits. For the primary combustion species, the Fuel Composition method is presented, which determines the EIs from the proportions of carbon, hydrogen and sulfur in the fuel. The set of methods concerning the estimation of $EINO_x$, EICO and EIHC include the ICAO reference method, the Boeing fuel flow method 2 (BFFM2), the DLR fuel flow method and the P3T3 method, in order of increasing fidelity. These methods interpolate engine performance data to determine emissions indices throughout the whole duration of a flight. Furthermore, methods are also presented to account for the remaining key emission species, such as the Derivative Factor method used to approximate the EI values for VOCs and non-methane HC (NMHC) throughout flight and the First Order Approximation method used to estimate PM emission indices. The choice of method generally depends on the emission species to be observed, the compromise between modelling resources and data availability, and the level of accuracy required.

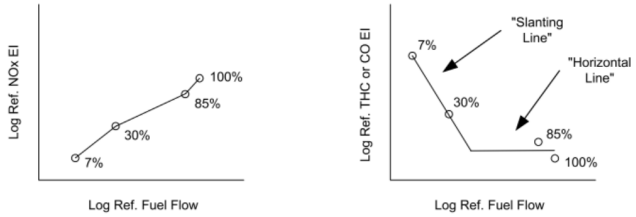

Figure 2. Example log-log plots of EI against fuel flow at reference conditions, as prescribed by the BFFM2 [11].

2.4.4. Emissions inventories and integration into large-scale climate models

The estimation of aircraft emissions for a specific flight involves the simulation of aircraft performance across the entire flight profile so as to estimate the fuel flow and engine operating conditions

throughout flight. Knowledge of fuel flows and engine performance characteristics permits the estimation of aircraft emissions, based on the coupling of empirical engine certification data and emissions modelling methods, which interpolate the data to determine the emissions at non-reference conditions. This emissions estimation procedure is commonly carried out on a regional and global scale to determine emissions from a whole range of flights, which are then stored in a so-called emissions inventory [**?**]. Aircraft emissions inventories collate data from all flights in the desired range and populate three-dimensional (3-D) latitude-longitude-altitude grid cells (e.g. 1°× 1°× 1000 ft) with total emissions quantities [12].

Aircraft emissions inventories are utilised to model the atmospheric effects of aviation, using a large-scale chemical transport model (CTM) or a climate-chemistry model (CCM), which captures the chemistry, physics and dynamics of the Earth-atmosphere system. Such models allow one to simulate the perturbation to the state of the atmosphere due to an input of emissions and, in turn, provide quantitative indicators that enable modellers to determine the resultant climate impact (e.g. concentrations of key chemical species, aerosol distribution, cloud processes etc.) [**?**]. However, one underlying issue with this conventional approach to aviation climate modelling, is that the use of gridded emissions data inherently assumes the instantaneous dispersion of emissions into the atmosphere [13]. In reality, the emissions released from aircraft are confined to an aircraft exhaust plume, which inhibits mixing with the surrounding atmosphere, for up to a day after emission. Throughout this time, a number of plume-scale processes occur, due to the elevated concentrations of emissions species in the plume, which are neglected in most regional and global aviation climate impact studies [14]. The following section covers the evolution of emissions throughout the lifetime of the aircraft exhaust plume and discusses the modelling approaches present in the literature which are implemented to represent and parametrise plume-scale effects in large-scale models of aviation's impact on the climate.

3. The dispersion of aircraft emissions and the aircraft exhaust plume

Following their expulsion into the free atmosphere throughout flight, aircraft exhaust gases are confined to a plume that undergoes a series of dynamical regimes (**jet**, **vortex**, **dispersion** and **diffusion** regimes), before becoming fully diluted in the surrounding air. The entrainment of emissions within the plume throughout these dynamical regimes leads to initial species concentrations that are several orders of magnitude higher than background levels [15], giving rise to a number of nonlinear chemical and microphysical effects. These plume-scale effects have considerable implications on the eventual chemical composition of the surrounding atmosphere and lead to the formation of aerosols and ice crystals in the aircraft wake. Therefore, inclusion of plume-scale effects is vital for high fidelity modelling of aviation's impact on the climate.

3.1. Plume-scale dynamical regimes

In order to accurately account for nonlinear effects experienced in the aircraft exhaust plume, one must first understand the dynamical response of the plume after combustion, to gauge the length and time scales over which aircraft emissions are entrained within it.

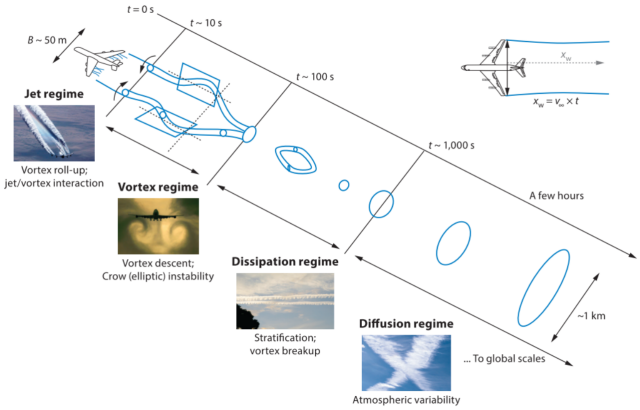

Figure 3. Aircraft exhaust plume dynamical regimes [12].

Once emitted from an aircraft's core engines, exhaust gases mix with engine bypass air and cool to around 300 K [3], forming an axisymmetric jet which rapidly diffuses into ambient air. This period, known as the **jet** regime, occurs over a timescale of around 1-20 s, with temperatures cooling to just above ambient throughout. Over the course of the jet regime, the airflow passing over the wings is diverted downwards to generate lift, thus creating a vortex sheet at the trailing edge of the aircraft. This vortex sheet rolls up into a pair of counter-rotating vortices which are shed at the wing tips. The evolving vortex pair then merge together and propagate downwards, due to their mutually induced downwash velocity, trapping the exhaust plume within their cores and signalling the beginning of the vortex regime.

Throughout the **vortex** regime, which occurs between 20 s and 2 minutes after combustion, the primary wake containing the vortices and trapped exhaust plume sinks by around 150–200 m, resulting in a slight temperature increase of 1–3 K, due to the adiabatic heating of exhaust constituents in the sinking vortices. Further to this, the organised vortical structure means the wake does not grow significantly during this time, and hence the concentrations of entrained chemical species remain relatively constant. The adiabatic heating of the exhaust does however lead to baroclinicity at the border between each vortex and the ambient air, which detrains some momentum, heat and exhaust constituents from the primary wake, to form a secondary wake. This secondary wake trails upwards as it is warmer than the surrounding ambient air, and it escapes the influence of the vortex structure, resulting in enhanced mixing with ambient air and thus experiences different chemical and microphysical processes compared to the primary wake [16].

Following this is the **dispersion** regime, in which the aircraft-induced dynamics subside due to the growth of Crow instability [17],

which dissipates and disintegrates the primary and secondary wake vortices [18]. The breakdown of the organised vortical structure and the production of turbulent motion leads to a sudden increase in the rate of entrainment between the exhaust plume and the ambient air by a factor of 10, therefore giving rise to a continuous decay of concentration and temperature within the plume. This regime lasts for 2–5 minutes after combustion.

Lastly, the plume undergoes its final dynamical event, known as the **diffusion** regime. This regime is characterised by the aircraft-induced dynamics becoming negligible (after about 6 minutes [19]), followed by the subsequent dominance of atmospheric processes in the spreading of the aircraft exhaust plume and its constituents. Atmospheric turbulence, radiation transport, stratification are examples of natural phenomena that contribute to the diffusion of the plume, with total dilution to ambient concentrations often occurring over timescales of 2–12 hours post emission. During this time, the plume may spread up to a few kilometres through atmospheric turbulence and shear in the ambient air, diluting the exhaust species over vast volumes of airspace [20].

3.2. Aircraft plume characteristics

The entrainment of aircraft emissions into the exhaust plume following release into the atmosphere has a considerable effect on the ensuing climate response, through nonlinear chemical and microphysical processing. The magnitude of plume processing is influenced by the spatial and temporal characteristics of the plume. This means that quantitative assessment and modelling of plume-scale effects on the climate requires knowledge of key plume properties such as the characteristic rate of mixing with ambient air, throughout the 4 dynamical regimes, and the lifetime over which the plume typically resides.

3.2.1. Dilution and rate of mixing

The eventual climate impact of aircraft emissions depends on the magnitude of nonlinear processing that occurs within the aircraft plume, and hence depends on the rate at which the plume expands and mixes with ambient air [20]. For this reason, analysis of plume-scale climate effects requires the estimation of plume dilution and mixing rates. In [21], empirical data was collated from over 70 aircraft exhaust plume encounters with research aircraft, to investigate the mixing rate of plumes throughout their typical lifetime. The characteristic property observed in this study is the plume dilution ratio, N, which is defined as the amount of air mass with which the exhaust plume generated from a unit mass of fuel burn, mixes with, per unit flight distance within the bulk of the plume.

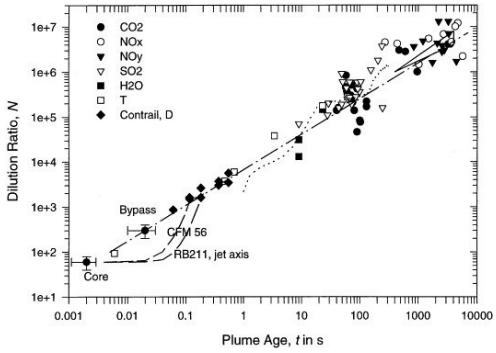

Figure 4. Dilution ratio against plume age derived from empirical data [21].

In figure 4, measured dilution ratios from the plume encounters are plotted against plume age. The data was generated by measuring the concentrations of a range of chemical sources across a variety of aircraft types between 0.001 to 10,000s. The significance of these findings is that, in spite of the diverse range of chemical species and aircraft types observed, throughout all four dynamical regimes, a relatively stable logarithmic relationship emerges between dilution ratio and increasing plume age. When interpolating the regression line fitted to the data in figure 4, the following equation can be obtained where N represents dilution ratio, t is plume age and t_0 serves as an arbitrary reference scale.

$$N = 7000(t/t_0)^{0.8},\ t_0 = 1s \tag{1}$$

It is evident from the figure however, that encounters with plumes older than 50–100 s tend to diverge from the line fit, indicating a reduction in accuracy of the logarithmic approximation over time. This is likely due to the transition from the organised vortex structure present in the vortex regime, to the turbulent dispersion regime, where more unpredictable atmospheric processes begin to take place and become the primary influence on the evolution of the plume. Therefore, this empirical model can only be used reliably up to the vortex regime. Beyond this, a Gaussian approximation to the distribution of species concentrations is typically employed, accounting for dispersion effects experienced at cruising altitudes, such as advection, gravitational sedimentation, anisotropic diffusion, wind shear and stable stratification [22]. See section **??** for more detail on the usage of Gaussian distributions and the two-dimensional diffusion equation in modelling aircraft plumes.

3.2.2. Plume lifetime

The lifetime of a plume is typically signified by the end of the diffusion regime and eventual return towards ambient background concentrations, around 2–12 h post emission. However, numerous distinct definitions have become apparent over the past few decades, which enable the concept of plume lifetime to be measured and used to determine the duration over which plume-scale processes should be accounted for when modelling the atmospheric effects of aviation. In [12], three definitions of plume lifetime are explored.

The first of these is the so-called "dispersion" time t_{ref} [13], defined as the time it takes for the plume to occupy the dimensions of a given reference area A_{ref}. This can be a useful metric to determine the time taken for a plume to become fully immersed in a known volume such as a latitude-longitude grid box of a global atmospheric model or the boundaries of a flight corridor. The second definition of plume lifetime is known as the "mixing" time t_{mix}, as [23**?** ,24]. This is the time in which the chemical conversion rate of NO_x in the plume becomes sufficiently close to that of the surrounding ambient air, falling below a very small threshold value. The dependency on the state of the background atmosphere means that this lifetime can change significantly with time and location. The final definition is from [14] where the lifetime t_l is determined by the exhaust concentrations dropping below a threshold mixing ratio and the excess exhaust mass dropping to zero.

The second lifetime definition, t_{mix}, is entirely dependent on the state of the background atmosphere, meaning the lifetime is subject to change significantly given a change in time and/or location of emission, as shown in figure 1 of [23]. Moreover, the first and third definitions not only vary with atmospheric conditions, but also depend on the threshold values set by the observer, meaning consistent thresholds must be maintained throughout a given study to maintain validity. Results from the aforementioned studies produced estimates of plume lifetime that lie in the range of 10–20 h. Given that plume lifetime and rate of mixing are calculable and measurable concepts, it is now possible to model the temporal and spatial scales of the chemically active plume, so as to investigate the extent to which nonlinear chemistry and microphysics influence the ensuing climate impact throughout the lifetime of the plume.

3.3. Plume-scale modelling

Convention amongst the climate modelling community is to assume instantaneous dispersion of aircraft emissions into the atmosphere, neglecting aircraft-induced dynamics and the presence of aircraft plumes, to which emissions are confined to for hours after release into the atmosphere. This approach therefore excludes plume-scale effects and thus leads to notable discrepancies in the chemical and physical response of the atmosphere in the model, compared to real life. To tackle the issue of neglected plume-scale effects, a number of plume modelling methods of varying fidelity have been theorised in the literature, and their outputs have been parametrised into global models to reduce uncertainties in the calculation of the climate impact of aviation.

3.3.1. Plume modelling methods

A common method found in [13] is known as the single plume (SP) model which approximates the time-evolving concentration field of an aircraft exhaust plume using a Gaussian distribution acting perpendicular to the flight path [25]. The SP model solves two sets of ordinary differential equations that describe the diffusion using horizontal (D_h), vertical (D_v) and shear (D_s) diffusion coefficients. One

set of equations is for the mean concentration inside the plume and the other is for the background concentration. From this, the plume volume and concentration can be deduced as a function of time, thus serving as input to atmospheric models in the form of plume mixing ratios and concentrations of key chemical species.

A generalisation to the SP model is the Multi-layered Plume model [12**?**]. This model discretises the concentration distribution in the radial direction into a number of concentric rings that each have a constant concentration equal to that of the mean concentration within the ring according to the Gaussian distribution. The primary benefit of this model over the SP model is the reduced computational demand from assuming discrete and homogeneous concentration rings, compared to the SP approach with a continuous concentration distribution.

Models such as the Aircraft Plume Chemistry, Emissions, and Microphysics Model (APCEMM) from [26] further increase the accuracy of the SP and Multi-layered Plume models by capturing additional effects that occur within the plume. This includes effects such as plume anisotropy and asymmetry which impact the eventual spatial distribution of the plume, and the inclusion of modelling of the microphysical processes that strongly influence contrail formation and persistence.

Finally, the plume dynamical evolution can be most accurately captured using high-resolution LESs over the entire lifetime of the plume. LESs can model dynamics on a scale of several millions of grid points for a few seconds to a few minutes of plume age, providing unmatched levels of accuracy at the cost of extremely high computational demand. For this reason, LESs are usually limited to case studies from which the data obtained can be used to derive and calibrate plume parametrisations for use in the lower fidelity methods [27].

3.3.2. Effective emissions and parametrisation into global models

- Attempt to parametrise into global models EEIs, ECFs, EERs
- Issues with resolving between plume and global models
- Nonlinear chemistry subsection in climate section will cover exact impact on chemical concs caused by plume effects (Ozone drop due to high conversion rate to reservoir in early plume)

4. Air traffic distribution

The previous section discussed the forces of flight and the generation and dispersion of aircraft emissions, from the perspective of a single aircraft. However, the state of the atmosphere is inhomogeneous with respect to space and time, meaning that the climate sensitivity to aircraft emissions differs considerably, depending on the time and location of their release. Therefore, to begin to understand the relationship between aircraft emissions and their resulting climate impact, one must first gain insight into the characteristic operation of aircraft within the wider air transportation system. Key factors that shape the distribution of air traffic, and hence aircraft emissions, include the management and control of air traffic flows and the obligation to meet geographical and temporal demand.

4.1. Air traffic management

The air traffic management (ATM) system is responsible for overseeing the network-wide implementation of safe, orderly and efficient air traffic flows, providing assistance to aircraft in transit from departure to destination aerodrome. It is the role of the air traffic control (ATC) team to manage and monitor air traffic in their respective airspace in real time, ensuring that the safety, order and efficiency of aircraft operations are maintained at all times [28]. This means that air traffic controllers must constantly monitor the state of the airspace, swiftly identifying and resolving any unfavourable circumstances by issuing the appropriate clearances or instructions to rectify the situation.

4.1.1. Air traffic safety

The inherent risk involved in the transportation of vast numbers of passengers at near transonic speeds through the upper atmosphere means that aviation safety is of paramount importance. A safe aircraft operation takes the path of least danger, primarily influenced by the need to avoid unfavourable atmospheric conditions and to prevent conflicts with other aircraft.

In-flight atmospheric conditions susceptible to icing, turbulence or the presence of hazardous convective weather can all be classified as unfavourable for aircraft, with the latter presenting the greatest constraint on aircraft routing [29]. The enhanced risk resulting from flight through weather-affected regions means that aircraft must reroute, leading to restrictions on available airspace and deviations from the optimal flight profile, thus increasing flight-times, fuel burn and delays [30].

The safety risks associated with aircraft-to-aircraft collisions necessitate air traffic controllers to impose safe separation standards between aircraft in the lateral, longitudinal and vertical direction, as specified in [31]. The stated minimum separation distances between aircraft are 5 nautical miles (NM) laterally, 20 NM longitudinally and 1,000 ft in the vertical direction under the most lenient scenarios. Enforcement of separation minima introduces a theoretical upper limit on airspace density within a fixed volume of airspace, in which a breach of separation in more than one direction, known as a conflict, must be resolved as quickly as possible.

The true upper limit on airspace density is determined by a parameter known as airspace capacity, defined as the maximum number of aircraft permitted in a region of airspace over a given time frame. The effective management of air traffic depends on the human cognition of air traffic controllers, to make difficult decisions and carry out complex tasks in a time-critical dynamic environment. As density and complexity levels of air traffic increase, so does the mental workload of the air traffic controller, up until a threshold level is reached where the controller can no longer safely handle the situation. This threshold mental workload is therefore a key determinant of airspace capacity, and is driven by the airspace situation, state of equipment being used, and the controller's own mental state [32]. To estimate capacity, controller workload models are used, which model ATC tasks

to determine a safe upper limit on workload. In [33], a macroscopic workload model is proposed which generalises ATC tasks into four distinct categories: background, transition, recurring and conflict tasks. This provides an objective basis for estimating capacity and enables the formulation of an analytical relationship between airspace capacity and sector volume, as seen in figure 5.

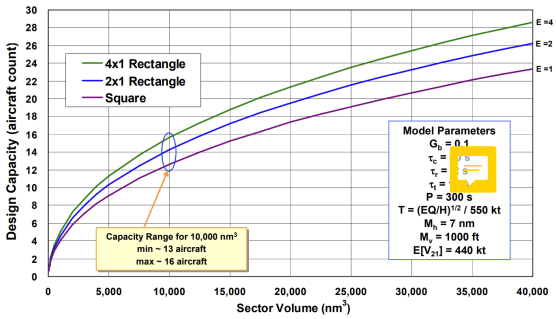

Figure 5. Aircraft capacity estimation against sector volume for a range of airspace scenarios [33].

4.1.2. Air traffic order

To keep air traffic flows organised within controlled airspace, aircraft are ordered to follow the traditional fixed-route air traffic network, limiting the possible trajectories flown and further restricting airspace availability. The air traffic network is constructed from four key airspace elements that facilitate the air traffic management process [28]:

- **airports/aerodromes** - an area of land or water intended to be used for the arrival, departure and surface movement of aircraft;
- **waypoints** - a specified geographical location used to define the flight path of an aircraft, representing either a navigational aid (navaid) or a reference coordinate that the aircraft must fly-by or fly-over;
- **airways** - a controlled portion of airspace established in the form of a corridor (usually 8-10NM wide) between two waypoints;
- **sectors** - a region of airspace managed by a single ATC team, stratified into various levels to accommodate a wide variety of traffic.

In [34], the notion of optimising air traffic flows for a given demand and capacity is explored, in which air traffic flows are represented using the four key elements. **Airports** represent the sources and sinks of the flow, **airways** are the arcs along which the flow travels, **waypoints** are the network nodes at which airways intersect, merge or diverge, and **sectors** are a collection of waypoints and contiguous segments of airways. Each airspace element has a corresponding capacity which is declared by the air traffic controller in charge of the airspace. If traffic volumes within respective airspace approach or exceed capacity levels, this can result in significant delays and congestion in the flow of air traffic, resulting in ATM efficiency losses, increased passenger dissatisfaction, and a greater environmental burden.

Controlled airspace is divided into the control zone (CTR), the terminal manoeuvring area (TMA) and en-route airspace. The control zone is the region of protected airspace in the immediate vicinity of an aerodrome, established to ensure the safe departure and arrival of aircraft [35]. The TMA is a larger control area situated above the control zone, which deals with aircraft in the landing and take-off (LTO) cycle, often serving as a junction for airways leading towards the control zone. Aircraft within this region must comply with so-called standard instrument departures (SIDs) and standard arrival routes (STARs) that are designated to a flight to minimise potential conflicts through the use of specific routing, speeds and altitudes. En-route airspace is defined as the volume of airspace outside terminal control areas, beginning at the termination of an SID and ending at the initiation of a STAR, encompassing the climb, cruise and descent phases of flight [36]. In en-route airspace, aircraft follow airways which are situated at a given flight level (FL), where flight levels are a measure of pressure altitude, expressed in hundreds of feet (e.g. FL 360 corresponds to a pressure altitude of 36,000 ft). Figure 6 portrays a typical vertical flight profile of an aircraft from departure to destination, under the constraints of controlled airspace.

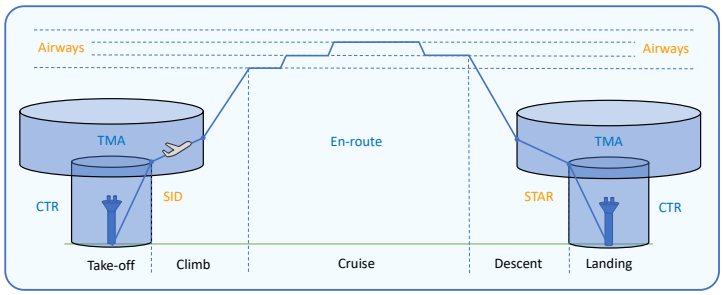

Figure 6. Typical aircraft trajectory subject to airspace constraints.

4.1.3. Air traffic efficiency

The third and final component of effective air traffic management is the optimisation of flight trajectories, subject to the prioritisation of safety and the compliance with the fixed-route airspace structure. Flight trajectory optimisation is an essential step in ensuring maximum airspace utilisation and efficiency, so that revenue is maximised and demand levels are sufficiently met. Trajectory optimisation is a multi-faceted problem, requiring consideration of nonlinear aircraft performance, wind and weather forecasts, payload, departure fuel load, reserve fuel load and ATM constraints that restrict aircraft operations and routing [37]. This requires an exhaustive assessment to be carried out at the flight planning stage, to test all possible combinations of route, payload, fuel load and operating approach, involving tens to hundreds of thousands of calculations per flight. The most optimal scenarios are then ranked in order of optimality, with the final route selected based on operator preference and/or the occurrence of unexpected circumstances, such as sudden adverse weather conditions or aircraft conflicts [38].

In an ideal airspace situation where the atmosphere is calm and constant; aircraft are not constrained to a fixed route; and there is no risk of conflict with other aircraft, the least-time and least-energy aircraft operation would be to fly the great-circle arc between departure and destination. The vertical profile of the aircraft would consist of a continuous climb out to the most efficient cruise altitude, then to cruise at constant speed, with the ability to cruise-climb continuously as the aircraft burns fuel and loses mass.

In reality, the true optimal route can deviate considerably from the great-circle arc, depending on the state of the atmosphere and the airspace situation along the route. Horizontal trajectory optimisation involves taking the path which minimises risk of bad weather encounters and collisions, abides by the fixed-route airspace structure, whilst also flying a route which is optimised with respect to wind and temperature. The magnitude and direction of wind and the localised variation in temperature experienced by the aircraft throughout flight, can have a drastic impact on route optimality, with tailwinds and colder temperature regions being favourable [39]. [40] found for a wide range of wind-optimal flight scenarios that domestic flights saved up to 3%, and international flights saving up to 10% on both fuel burn and travel time, despite flying longer routes. Trajectory optimisation in the vertical direction involves climbing to the optimum cruise altitude where air density is low so drag is minimised, whilst maintaining sufficient airflow to provide adequate thrust and lift to achieve steady level flight. In fixed-route airspace however, the aircraft must conform to flight level allocations, meaning that as the aircraft climbs as it burns fuel, it must remain at allocated flight levels, further condensing air traffic and its corresponding emissions into narrow bands of altitude.

4.2. Aviation demand

Flight routes are constrained by the need to avoid hazardous situations, abide by ATC standards and optimise aircraft operations, however another factor which significantly affects air traffic distribution is aviation demand. There are inconsistencies in the levels of demand for aviation both geographically and temporally, depending on the demographic of the area and the preferences of those who do fly.

4.2.1. Global air traffic and emissions distribution

The nature of air traffic and emissions distribution was investigated in [41] where a range of global aircraft emissions datasets are compared (NASA-Boeing 1992, NASA-Boeing 1999, QUANTIFY 2000, Aero2k 2002, AEDT 2006 and aviation fuel usage estimates from the International Energy Agency) to show distribution patterns in the latitudinal, longitudinal and vertical sense. Further to this, temporal variations with respect to both the diurnal (time of day) and seasonal (time of year) cycles are explored.

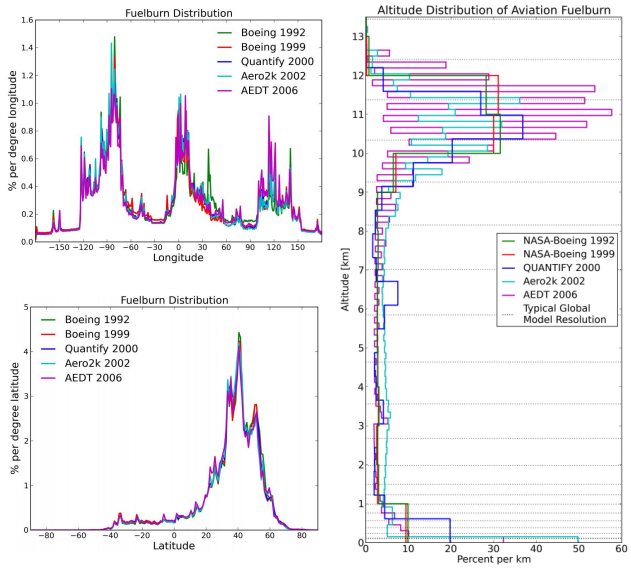

Figure 7. Spatial (latitude, longitude and altitude) distribution of global aviation emissions from a range of aircraft emissions datasets [41].

Figure 7 shows the spatial distribution of fuel burn across the range of datasets in the longitudinal, latitudinal and vertical directions. The longitudinal distribution shows three emissions peaks around the densely-populated regions of the US, Europe and East Asia, with the largest situated above the North American land mass. It is evident in the latitudinal distribution, that the Northern Hemisphere dominates, with a strong peak in the northern mid-latitudes that appears due to high volumes of air traffic above the US and Europe, as well as along the connecting region of airspace, the North Atlantic flight corridor (NAFC). Contrarily, there are almost no emissions present in southern latitudes below 40°S, with the region between 40°S and the equator constituting only a small percentage. The altitudinal distribution on the other hand, experiences emissions peaks around both the low altitude LTO area and the high-altitude cruising regions between 9 to 13 km, with relatively low emission intensities at mid-altitudes. Furthermore, the peak around cruising altitude is discretised into peaks every other flight level, due to the vertical separation constraints and the allocation of aircraft to specific flight levels, thus owing to further increases in emissions intensities at these altitudes.

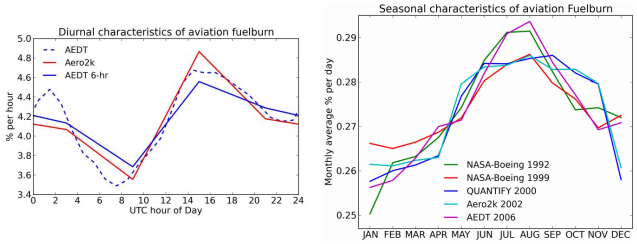

Figure 8. Temporal (diurnal and seasonal) distribution of global aviation emissions from a range of aircraft emissions datasets [41].

The temporal variation of atmospheric parameters evident in figure 8 (e.g. background concentrations and reaction rates) means that the climate sensitivity to aircraft emissions is highly dependent on when the emission is released. Therefore, understanding the temporal emissions distribution with respect to the diurnal and seasonal trends is crucial. The diurnal cycle of global aviation fuel burn, as seen on the left hand side of figure 8 displays a peak at around 15:00UTC, which decreases through the night until around 09:00UTC where total fuel burn begins to increase again. With regards to seasonal variation, there is significant variance between emissions datasets, however in general, all display a wintertime minimum between December and January, and a summertime maximum between June and September.

4.2.2. Local air traffic and emissions distribution

Due to the fixed-route nature of airspace, aircraft tend to fly along common airways or flight corridors, and pass common waypoints along their journey, leading to exceptionally high flux densities of aircraft through these regions at peak times. This has implications on the nonlinear chemical and physical effects occurring at the plume scale, due to the intersection of aircraft plumes and the elevated exhaust gas concentrations entrained within them. A prime example of a high-density airspace region is the NAFC, made up of a series of tracks that aircraft traversing the North Atlantic must follow, updated daily to allow for convective weather avoidance, tracking of the North Atlantic Jet Stream and favourable tailwinds to maximise efficiency [42]. The annually-averaged number of aircraft traversing the NAFC per day has increased from 800 in 1997 [43] to around 2,500 in recent years [35], owing to the tripling of passenger demand since then [44]. With North Atlantic air traffic being confined to a limited number of tracks (usually 3 or 4), it can be assumed that aircraft separation distances and airspace capacities are pushed to their limit on a regular basis along this flight corridor.

Previous experimental work on air traffic emissions in the NAFC was carried out in the late 1990's, through campaigns such as the Pollution from Aircraft Emissions in the North Atlantic Flight Corridor (POLINAT) and Subsonic Assessment Ozone and Nitrogen Oxide Experiment (SONEX) [45]. At least 20 follow up papers were published following these campaigns, in which POLINAT/SONEX data are utilised to provide insight on a number of major scientific issues [46]. A noteworthy publication with regards to localised emissions impacts is [47], which carries out an in-situ investigation of air traffic emissions signatures (nitrogen oxides (NO_x), sulfur dioxide (SO_2) and cloud condensation nuclei (CN)) in the NAFC using experimental data from a POLINAT research flight. The research aircraft flew perpendicular to the major eastbound corridor tracks and took measurements of various chemical concentration fields and meteorological parameters throughout. The results show that the superposition of aircraft exhaust plumes led to peak concentrations of NO_x, SO_2 and CN above background levels by factors of 30, 5 and 3, respectively. This is because plume dispersion timescales greatly exceed the daily frequency with which aircraft emissions are input into the flight corridor, resulting in

an inhomogeneous concentration field with narrow and sharp peaks over a relatively low and smooth background level [45].

The management and optimisation of air traffic directly influences the distribution of aircraft, and hence their associated emissions, throughout the atmosphere at cruising altitudes. The importance of safety, order and efficiency in the air traffic management process and the characteristics of global and local air traffic flows have been discussed. The following section will explore the atmospheric response to the input of aviation emissions on a global and local scale, through evaluation of the climate forcing mechanisms that result from emissions and analysis of their relative global warming contributions. Further to this, the nonlinear chemistry and microphysics within the exhaust plume is covered in great detail.

5. The climate impact of aviation

5.1. Atmospheric chemistry in the UTLS

As figure 7 suggests, the vast majority of aviation fuelburn and hence aviation emissions, occur between 9 and 13km altitude. The region of the atmosphere encompassing this volume of airspace is known as the Upper Troposphere and Lower Stratosphere (UTLS), with around 20-40% of total aircraft emissions being released in the LS [48]. The greenhouse effect due to the release of chemically-active substances in the UTLS is considerably greater than that of emissions at the surface, due to the increased sensitivity of the climate at these altitudes. The climate in the UTLS is more sensitive due to increased residence times of pollutants, lower background concentrations meaning emissions have a greater influence on the chemistry, lower temperatures, and a higher radiative efficiency **??**. The climate effects associated with water vapour and NO_x emissions are particularly sensitive to the atmospheric conditions of the UTLS. Water vapour emissions released into the sufficiently cold and humid conditions of the upper atmosphere form condensation trails, which trap heat more effectively than they reflect inbound solar radiation, leading to a net global warming effect. Moreover, NO_x emissions constitute a 30 times greater climate impact compared to equivalent surface emissions, due to the absence of direct deposition and slower conversion to stable reservoir species at aircraft cruising altitudes [**?**].

With the enhanced climate sensitivity of the UTLS and the highly variable chemical and meteorological state of the atmosphere at these altitudes, the climate impact induced by an aircraft depends not only on the mass of emissions it releases, but also on the time and location of their release. Therefore, aircraft emissions climate effects are spatio-temporally sensitive and require comprehensive climate metrics to quantify their atmospheric effects.

5.2. Radiative forcing of aircraft emissions

The most common climate metric used to compare the magnitudes of climate impact from a range of emission species is radiative forcing (RF). RF is defined as the perturbation to the net energy balance of the Earth-atmosphere system due to natural or anthropogenic factors of climate change, measured in watts per square metre [W/m2]

[49]. The emission of harmful chemical species into the UTLS, as is the case for aviation, induces a number of climate forcing mechanisms that exhibit a radiative forcing effec[50] presents an updated analysis of the global effective radiative forcing (ERF) contributions for aviation-induced climate change. ERF is a newly proposed climate modelling framework that builds upon the RF concept by removing rapid atmospheric adjustments that bear no relation to the long-term surface temperature response that occurs over decadal timescales. ERF serves as a more suitable equivalency metric to compare the global warming response of heterogeneously distributed short-lived climate forcers and uniformly distributed long-lived climate forcers. Figure 9 displays the ERF and RF contributions for each of the key aviation-induced climate forcers.

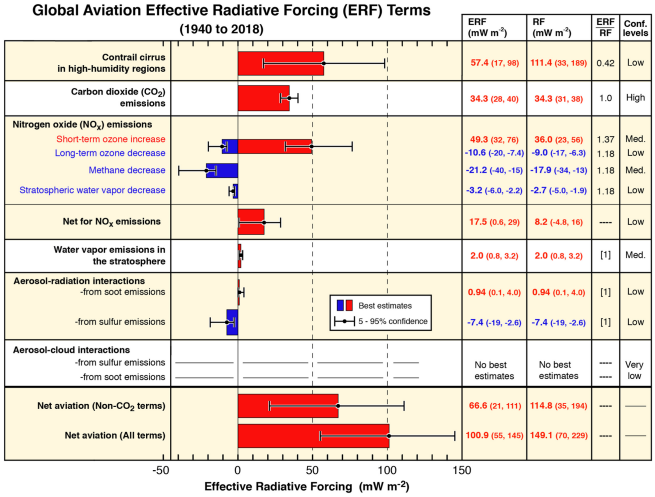

Figure 9. Radiative forcing contributions from global aviation between 2000 and 2018 [50].

5.2.1. CO_2

The RF of aviation CO2 emissions is direct and well understood. Due to its thermodynamic and photochemical stability, CO2 has a relatively long atmospheric lifetime on the order of 100 to 1,000 years. This means that aviation CO2 emitted into the atmosphere simply serves to increase its atmospheric concentration, leading to the eventual distribution over global spatial scales and a steady, uniform increase in the planetary greenhouse effect[51]e ubiquitous and intuitive nature of CO_2-related warming deems it a suitable benchmark to compare warming from non-CO_2 climate forcers against.

5.2.2. Contrail cirrus

Water vapour and particulate emissions released from jet-powered aircraft in sufficiently cold and humid conditions give rise to the generation of anthropogenic vapour trails, known as contrails. Such trails often have a significant level of opacity and occur at high altitudes, tending to absorb outbound terrestrial radiation more efficiently than they reflect inbound solar radiation, thus inducing a net global heating effect. The extent of contrail-related warming is highly dependent on the ambient conditions of the surrounding atmosphere – in particular,

773 contrails generated in regions which are supersaturated with respect
774 to ice are thought to create the greatest warming effect. The ice crystals
775 they are composed of grow with age and spread over vast expanses
776 of the atmosphere, often leading to the formation of additional cirrus
777 clouds, or the consolidation of existing ones, at high-altitudes in the
778 upper atmosphere.

779 #### 5.2.3. Net-NO_x

780 Tropospheric chemistry is dominated by ozone (O_3), a potent
781 greenhouse gas which contributes to climate change and air quality
782 issues. O_3 is an oxidant in its own right, reacting with reactive volatile
783 organic compounds (VOCs, see later) but is the precursor to the OH
784 radical, which is known as the chemical detergent of the lower at-
785 mosphere. The OH radical reacts with VOCs and allows them to be
786 oxidised and removed from the atmosphere. Photolysis of ozone (ab-
787 sorption of sunlight in the UV region 290-330 nm and the breaking
788 of an O-O bond) starts the process of OH production, depicted by
789 reaction (1), where hv denotes a photon of light;

$$O_3 + hv \longrightarrow O^* + O_2 \quad (2)$$

790 Reaction (1) makes a reactive oxygen atom O*, that can either
791 collide with N2 or O2 molecules (denoted as M) and be quenched to
792 ground state O atoms in reaction (2)

$$O^* + M \longrightarrow O + M \quad (3)$$

793 Or it can react with water to form HO radicals

$$O^* + H_2O \longrightarrow OH + OH \quad (4)$$

794 OH radicals can then participate in chemical cycles that preserve
795 levels but also remove pollutants, CO, in the following examples.
796 First, under clean conditions (low NOx = NO and NO2) the following
797 scheme (1) takes place:

$$OH + CO \longrightarrow H + CO_2 \quad (5)$$

$$H + O_2 + M \longrightarrow HO_2 + M \quad (6)$$

$$HO_2 + O_3 \longrightarrow OH + 2\,O_2 \quad (7)$$

798 Net reaction $CO + O_3 \longrightarrow CO_2 + O_2$
799 Here, ozone is removed and CO is oxidised to form CO_2, which,
800 in a pre-industrial world, was taken up by plants and the oceans
801 on relatively short timescales. This clean condition scheme removes
802 pollutants and keeps ozone levels under control. However, industrial
803 activity through fossil fuel combustion has increased levels of NO_x in
804 the atmosphere, changing from scheme (1) to scheme (2):

$$OH + CO \longrightarrow H + CO_2 \quad (8)$$

$$H + O_2 + M \longrightarrow HO_2 + M \quad (9)$$

$$HO_2 + NO \longrightarrow OH + NO_2 \quad (10)$$

$$NO_2 + hv \longrightarrow NO + O \quad (11)$$

$$O + O_2 + M \longrightarrow O_3 + M \quad (12)$$

Net reaction: $CO + 2\,O_2 \longrightarrow CO_2 + O_3$

Now, ozone is formed as CO is oxidised, and one can assume that adding more NO_x would further increase ozone production. However, if NO and NO_2 levels surpass a threshold, they can compete with VOC for reaction with OH radicals:

$$OH + NO + M \longrightarrow HONO + M \quad (13)$$

$$OH + NO_2 + M \longrightarrow HNO_3 + M \quad (14)$$

Reactions (13) and (14) are called termination reactions, removing radicals from the atmosphere and preventing O_3 formation. In polluted environments, OH collapse can occur, and so ...

5.2.4. Stratospheric water vapour

5.2.5. Aerosol effects

5.3. Nonlinear chemistry and microphysics in the aircraft exhaust plume

6. Plume superposition

Following expulsion into the free atmosphere, exhaust species become entrained in the aircraft wake, forming a plume of elevated chemical concentrations which persist for 2 to 12 hours **??**, before fully dispersing into ambient air. The build-up of non-CO2 emissions in the plume give rise to a number of nonlinear chemical and microphysical effects, which influence the ensuing atmospheric response by altering the net production rates of radiatively active gases and affecting contrail formation and persistence. It is often the case however, that in large-scale atmospheric models, emissions are instantaneously diluted into the volume of the smallest resolved grid cell, with dimensions according to the model's spatial resolution. The instantaneous dilution (ID) approach neglects the plume-scale processes, thus leading to discrepancies in the calculated climate response such as the overestimation of O3 production, CH4 and CO destruction, and the increased rate of NOx conversion to nitrogen reservoir species **??**. Furthermore, it is stated in **??** that the formation of ice in aircraft exhaust plumes may result in additional heterogeneous chemical reactions, that are not captured in global atmospheric models.

6.1. Plume superposition

6.2. Atmospheric response to plume superposition

In **??** the notion of plume superposition and the extent to which it influences the atmospheric response was explored, by comparing

results from an expanding plume model against an atmospheric model which assumes instant dilution. The analysis was carried out firstly on a single aircraft at cruise altitude, then on four aircraft flying in the same direction each separated by 1 hr. Observing the single aircraft's plume 10 hrs after emission, it was found that the instantaneous dilution approach overestimated O3 production by 33%, CH4 destruction by 30% and CO destruction by 32%. When observing the response due to the four overlapping plumes however, the overestimation of O3 production increases to 77%, CH4 destruction to 68% and CO destruction to 74%. The marked difference in measured response for four overlapping plumes compared to a single plume serves as evidence that emissions saturation in superimposed plumes can significantly alter the chemical response of the atmosphere. However, further work needs to be done to clarify the direction and magnitude of the net change in climate impact resulting from these changes to the chemical composition. Moreover, the sensitivity of the chemical and climate response to plume superposition needs to be tested for a range of aircraft transit frequencies and ambient atmospheric conditions, so as to build up a visual representation over the phase space of the atmosphere. In addition to chemical changes in the atmosphere, plume overlap can also influence the formation and persistence of aircraft contrails and the subsequent generation of aviation-induced cirrus clouds. **??** explored the effect of recurrent water vapour emission on contrail formation and persistence at typical aircraft cruising altitudes. It was discovered that continual contrail generation actually leads to dehydration of the surrounding atmosphere and a diminishing radiative forcing effect of 15% in the affected areas. This outcome provides further impetus to explore the potential effects of plume superposition on the global warming induced by aviation.

7. Mitigation potential

7.1. Formation flight

Formation flight involves the flight of two or more aircraft in aerodynamic formation, with the follower aircraft positioned in the smooth updraft of the leader aircraft's wake, reducing required lift and thrust, hence reducing fuel and CO2 emissions by 5-8% per trip **??**. A fortuitous outcome of formation flight is however, the saturation of emissions in the trailing exhaust plumes, which can lead to the aforementioned nonlinear chemical and microphysical response that reduces ozone and contrail formation. The non-CO2 climate effects of a twin-aircraft formation flight are observed in **??**, where a climate model was used to determine the changes in NOx-related ozone production and contrail formation processes. The case study found that, despite a 1-3% increase in flown distance, CO2 was reduced by 6% and NOx was reduced by 11%. This resulted in a 5% reduction in ozone production efficiency due to NOx saturation and a 48% contrail reduction due to mutual competition for available water vapour, resulting in a total climate impact reduction of approximately 23%. While part of the alleviated climate impact can be related to the decrease in total emissions due to wake energy retrieval of the follower aircraft, there is also further emphasis due to the saturation of emissions in the

overlapping plumes of both aircraft involved. This demonstrates great potential for reducing both CO2- and non-CO2-induced climate effects from aviation, if such a scheme were to be carried out on a global scale.

7.2. Climate-optimal aircraft routing

Fleet-wide implementation of formation flight would however, pose a number of research obstacles, that must be overcome to maximise its cost-benefit potential, whilst ensuring the safe and orderly operation of aircraft in controlled airspace. Optimising aircraft trajectories to minimise fuel burn requires the consideration of nonlinear aircraft performance, wind and weather, payload, fuel load, and constraints set out by air traffic control **??**. Formation flight adds another variable to the fuel burn optimisation problem, maximising the time spent flying in formation whilst minimising deviation from the true optimal route. This is a research topic covered extensively in the literature **??**. Optimising formation flight trajectories to minimise climate impact on the other hand, is a relatively novel concept, which requires deeper understanding of the sensitivity of the climate response to emissions under a range of different atmospheric states.

7.3. Alternative propulsion technologies

8. Plume-scale processes

Following expulsion into the free atmosphere, exhaust species become entrained in the aircraft wake, forming a plume of elevated chemical concentrations which persist for 2 to 12 hours **??**, before fully dispersing into ambient air. The build-up of non-CO2 emissions in the plume give rise to a number of nonlinear chemical and microphysical effects, which influence the ensuing atmospheric response by altering the net production rates of radiatively active gases and affecting contrail formation and persistence. It is often the case however, that in large-scale atmospheric models, emissions are instantaneously diluted into the volume of the smallest resolved grid cell, with dimensions according to the model's spatial resolution. The instantaneous dilution (ID) approach neglects the plume-scale processes, thus leading to discrepancies in the calculated climate response such as the overestimation of O3 production, CH4 and CO destruction, and the increased rate of NOx conversion to nitrogen reservoir species **??**. Furthermore, it is stated in **??** that the formation of ice in aircraft exhaust plumes may result in additional heterogeneous chemical reactions, that are not captured in global atmospheric models.

8.1. Plume superposition

8.2. Atmospheric response to plume superposition

In **??**, the notion of plume superposition and the extent to which it influences the atmospheric response was explored, by comparing results from an expanding plume model against an atmospheric model which assumes instant dilution. The analysis was carried out firstly on a single aircraft at cruise altitude, then on four aircraft flying in the same direction each separated by 1 hr. Observing the single aircraft's plume 10 hrs after emission, it was found that the instantaneous dilution approach overestimated O3 production by 33%, CH4 destruction

by 30% and CO destruction by 32%. When observing the response due to the four overlapping plumes however, the overestimation of O3 production increases to 77%, CH4 destruction to 68% and CO destruction to 74%. The marked difference in measured response for four overlapping plumes compared to a single plume serves as evidence that emissions saturation in superimposed plumes can significantly alter the chemical response of the atmosphere. However, further work needs to be done to clarify the direction and magnitude of the net change in climate impact resulting from these changes to the chemical composition. Moreover, the sensitivity of the chemical and climate response to plume superposition needs to be tested for a range of aircraft transit frequencies and ambient atmospheric conditions, so as to build up a visual representation over the phase space of the atmosphere. In addition to chemical changes in the atmosphere, plume overlap can also influence the formation and persistence of aircraft contrails and the subsequent generation of aviation-induced cirrus clouds. **??** explored the effect of recurrent water vapour emission on contrail formation and persistence at typical aircraft cruising altitudes. It was discovered that continual contrail generation actually leads to dehydration of the surrounding atmosphere and a diminishing radiative forcing effect of 15% in the affected areas. This outcome provides further impetus to explore the potential effects of plume superposition on the global warming induced by aviation.

1. Gössling, S.; Humpe, A. The global scale, distribution and growth of aviation: Implications for climate change. *Global Environmental Change* **2020**, *65*. doi:10.1016/j.gloenvcha.2020.102194.
2. Anderson, J.D. *Aircraft perfomance and design*; Vol. 358, 1999; pp. 1–41.
3. Brasseur, G.; Cox, R.; Hauglustaine, D.; Isaksen, I.; Lelieveld, J.; Lister, D.; Sausen, R.; Schumann, U.; Wahner, A.; Wiesen, P. European scientific assessment of the atmospheric effects of aircraft emissions. *Atmospheric Environment* **1998**, *32*, 2329–2418. doi:10.1016/S1352-2310(97)00486-X.
4. Döpelheuer, A. Aircraft emission parameter modelling. *Air & Space Europe* **2000**, *2*, 34–37. doi:10.1016/S1290-0958(00)80060-X.
5. Dopelheuer, A.; Lecht, M. Influence of engine performance on emission characteristics. *RTO-Symposium of AVT on Gas Turbine Engine Combustion, Emissions and Alternative Fuels* **1998**.
6. Nuic, A.; Poles, D.; Mouillet, V. BADA: An advanced aircraft performance model for present and future ATM systems. *International Journal of Adaptive Control and Signal Processing* **2010**, *24*, 850–866. doi: 10.1002/acs.1176.
7. Lissys Ltd. Piano-X Aircraft Emissions and Performance User's Guide. Technical report, Lissys Ltd, 2008.
8. Administration, F.A. Aviation Environment Design Tool (AEDT) 2a: Technical Manual, Version 3c. Technical report, FAA, 2020.
9. International Civil Aviation Organization (ICAO) Committee on Aviation Environmental Protection (CAEP). *ICAO Aircraft Engine Emissions Databank*, 28 ed.; 2021.
10. International Civil Aviation Organization (ICAO). Annex 16 to the Convention on International Civil Aviation–Volume I–Aircraft Noise. *Icao* **2008**, *552*.

11. SAE Aerospace. *Procedure for the Calculation of Aircraft Emissions*, 2009. doi:https://doi.org/10.4271/AIR5715.
12. Paoli, R.; Cariolle, D.; Sausen, R. Review of effective emissions modeling and computation. *Geoscientific Model Development* **2011**, *4*, 643–667. doi: 10.5194/gmd-4-643-2011.
13. Petry, H.; Hendricks, J.; Möllhoff, M.; Lippert, E.; Meier, A.; Ebel, A.; Sausen, R. Chemical conversion of subsonic aircraft emissions in the dispersing plume: Calculation of effective emission indices. *Journal of Geophysical Research: Atmospheres* **1998**, *103*, 5759–5772. doi: 10.1029/97JD03749.
14. Cariolle, D.; Caro, D.; Paoli, R.; Hauglustaine, D.A.; Cuénot, B.; Cozic, A.; Paugam, R. Parameterization of plume chemistry into large-scale atmospheric models: Application to aircraft NOx emissions. *Journal of Geophysical Research Atmospheres* **2009**, *114*, 1–21. doi: 10.1029/2009JD011873.
15. Danilin, M.Y.; Ebel, A.; Elbern, H.; Petry, H. Evolution of the concentrations of trace species in an aircraft plume: trajectory study. *Journal of Geophysical Research* **1994**, *99*. doi:10.1029/94jd01820.
16. Gerz, T.; Dürbeck, T.; Konopka, P. Transport and effective diffusion of aircraft emissions. *Journal of Geophysical Research Atmospheres* **1998**, *103*, 25905–25913. doi:10.1029/98JD02282.
17. Crow, S.C. Stability Theory for a Pair of Trailing Vortices. *AIAA Journal* **1970**, *8*, 2172–2179. doi:10.2514/3.6083.
18. Paoli, R.; Shariff, K. Contrail Modeling and Simulation. *Annual Review of Fluid Mechanics* **2016**, *48*, 393–427. doi: 10.1146/annurev-fluid-010814-013619.
19. Unterstrasser, S.; Paoli, R.; Sölch, I.; Kühnlein, C.; Gerz, T. Dimension of aircraft exhaust plumes at cruise conditions: Effect of wake vortices. *Atmospheric Chemistry and Physics* **2014**, *14*, 2713–2733. doi: 10.5194/acp-14-2713-2014.
20. Schumann, U.; Konopka, P.; Baumann, R.; Busen, R.; Gerz, T.; Schlager, H.; Schulte, P.; Volkert, H. Estimate of diffusion parameters of aircraft exhaust plumes near the tropopause from nitric oxide and turbulence measurements. *Journal of Geophysical Research* **1995**, *100*, 14147–14162.
21. Schumann, U.; Schlager, H.; Arnold, F.; Baumann, R.; Haschberger, P.; Klemm, O. Dilution of aircraft exhaust plumes at cruise altitudes. *Atmospheric Environment* **1998**, *32*, 3097–3103. doi: 10.1016/S1352-2310(97)00455-X.
22. Konopka, P. Analytical Gaussian Solutions for Anisotropie Diffusion in a Linear Shear Flow. *Journal of Non-Equilibrium Thermodynamics* **1995**, *20*. doi:10.1515/jnet.1995.20.1.78.
23. Karol, I.L.; Ozolin, Y.E.; Kiselev, A.A.; Rozanov, E.V. Plume Transformation Index (PTI) of the Subsonic Aircraft Exhausts and their Dependence on the External Conditions **2000**. *27*, 373–376.
24. Kraabøl, A.G.; Konopka, P.; Stordal, F.; Schlager, H. Modelling chemistry in aircraft plumes 1: Comparison with observations and evaluation of a layered approach. *Atmospheric Environment* **2000**, *34*, 3939–3950. doi: 10.1016/S1352-2310(00)00156-4.
25. Vohralik, P.F.; Randeniya, L.K.; Plumb, I.C.; Baughcum, S.L. Effect of plume processes on aircraft impact. *Journal of Geophysical Research Atmospheres* **2008**, *113*, 1–21. doi:10.1029/2007JD008982.
26. Fritz, T.M.; Eastham, S.D.; Speth, R.L.; Barrett, S.R. The role of plume-scale processes in long-term impacts of aircraft emissions. *Atmospheric Chemistry and Physics* **2020**, *20*, 5697–5727. doi: 10.5194/acp-20-5697-2020.

27. Lewellen, D.C.; Lewellen, W.S.; Poole, L.R.; DeCoursey, R.J.; Hansen, G.M.; Hostetler, C.A.; Kent, G.S. Large-eddy simulations and lidar measurements of vortex-pair breakup in aircraft wakes. *AIAA Journal* **1998**, *36*, 1439–1445. doi:10.2514/2.535.
28. Secretariat General. *Annex 11 Environment*; Number July, 2016; p. 18.
29. Krozel, J.; Mitchell, J.S.; Polishchuk, V.; Prete, J. Capacity estimation for airspaces with convective weather constraints. *Collection of Technical Papers - AIAA Guidance, Navigation, and Control Conference 2007* **2007**, *2*, 1518–1532. doi:10.2514/6.2007-6451.
30. Federal Aviation Administration. FAQ: Weather Delay, 2021.
31. International Civil Aviation Authority. *Doc 4444 - Air Traffic Management - Procedures for Air Navigation Services*, 16 ed.; 2016.
32. Majumdar, A.; Ochieng, W.Y.; McAuley, G.; Lenzi, J.M.; Lepadatu, C. The factors affecting airspace capacity in Europe: A cross-sectional time-series analysis using simulated controller workload data. *Journal of Navigation* **2004**, *57*, 385–405. doi:10.1017/S0373463304002863.
33. Welch, J.D.; Andrews, J.W.; Martin, B.D.; Sridhar, B. Macroscopic workload model for estimating en route sector capacity. *Proceedings of the 7th USA/Europe Air Traffic Management Research and Development Seminar, ATM 2007* **2007**, pp. 94–103.
34. The Flow Management Problem in Air Traffic Control. In *Flow control of congested networks*; Springer-Verlag Berlin Heidelberg, 1987; Vol. 38, pp. 269–288.
35. Brunton, J. North Atlantic Skies – The gateway to Europe. https://nats.aero/blog/2014/06/north-atlantic-skies-gateway-europe/, 2014.
36. US Federal Aviation Administration (FAA)., En Route Operations. In *Instrument Procedures Handbook*; 2017; chapter 2.
37. Soler, M.; Olivares, A.; Staffetti, E. Multiphase optimal control framework for commercial aircraft four-dimensional flight-planning problems. *Journal of Aircraft* **2015**, *52*, 274–286. doi:10.2514/1.C032697.
38. Altus, S. Effective Flight Plans Can Help Airlines Economize. https://www.boeing.com/commercial/aeromagazine/articles/qtr_03_09/pdfs/AERO_Q309_article08.pdf.
39. Murrieta-Mendoza, A.; Botez, R. Lateral navigation optimization considering winds and temperatures for fixed altitude cruise using Dijsktra's algorithm. *ASME International Mechanical Engineering Congress and Exposition, Proceedings (IMECE)* **2014**, *1*, 1–9. doi:10.1115/IMECE2014-37570.
40. Ng, H.K.; Sridhar, B.; Grabbe, S. A practical approach for optimizing aircraft trajectories in winds. 2012 IEEE/AIAA 31st Digital Avionics Systems Conference (DASC). IEEE, 2012.
41. Olsen, S.C.; Wuebbles, D.J.; Owen, B. Comparison of global 3-D aviation emissions datasets. *Atmospheric Chemistry and Physics* **2013**, *13*, 429–441. doi:10.5194/acp-13-429-2013.
42. North Atlantic Tracks - Flight Plan database. https://flightplandatabase.com/nav/NATS.
43. Kärcher, B.; Meilinger, S.K. Perturbation of the aerosol layer by aviation-produced aerosols: A parametrization of plume processes. *Geophysical Research Letters* **1998**, *25*, 4465–4468. doi:10.1029/1998GL900183.
44. Air transport, passengers carried. https://data.worldbank.org/indicator/IS.AIR.PSGR.
45. Schumann, U.; Schlager, H.; Arnold, F.; Ovarlez, J.; Kelder, H.; Hov.; Hayman, G.; Isaksen, I.S.; Staehelin, J.; Whitefield, P.D. Pollution from aircraft emissions in the North Atlantic flight corridor: Overview on the

POLINAT projects. *Journal of Geophysical Research Atmospheres* **2000**, *105*, 3605–3631. doi:10.1029/1999JD900941.
46. Thompson, A.M.; Singh, H.B.; Schlager, H. Introduction to special section: Subsonic assessment ozone and nitrogen oxide experiment (SONEX) and Pollution from aircraft emissions in the north atlantic flight corridor (POLINAT 2). *Journal of Geophysical Research: Atmospheres* **2000**, *105*, 3595–3603. doi:10.1029/2000JD900012.
47. Schlager, H.; Konopka, P.; Schulte, P.; Schumann, U.; Ziereis, H.; Arnold, F.; Klemm, M.; Hagen, D.E.; Whitefield, P.D.; Ovarlez, J. In situ observations of air traffic emission signatures in the North Atlantic flight corridor. *Journal of Geophysical Research* **1997**, *102*, 10739–10750. doi: 10.1029/96JD03748.
48. Penner, J.; Lister, D.; Griggs, D.; Dokken, D.; McFarland, M., Aviation and the Global Atmosphere; Cambridge University Press, 1999; chapter 2.
49. Fuglestvedt, J.S.; Berntsen, T.K.; Godal, O.; Sausen, R.; Shine, K.P.; Skodvin, T. Metrics of climate change: Assessing radiative forcing and emission indices. *Climatic Change* **2003**, *58*, 267–331. doi: 10.1023/A:1023905326842.
50. Lee, D.; Fahey, D.; Skowron, A.; Allen, M.; Burkhardt, U.; Chen, Q.; Doherty, S.; Freeman, S.; Forster, P.; Fuglestvedt, J.; Gettelman, A.; De León, R.; Lim, L.; Lund, M.; Millar, R.; Owen, B.; Penner, J.; Pitari, G.; Prather, M.; Sausen, R.; Wilcox, L. The contribution of global aviation to anthropogenic climate forcing for 2000 to 2018. *Atmospheric Environment* **2021**, *244*, 117834. doi:10.1016/j.atmosenv.2020.117834.

Author Contributions: For research articles with several authors, a short paragraph specifying their individual contributions must be provided. The following statements should be used "Conceptualization, X.X. and Y.Y.; methodology, X.X.; software, X.X.; validation, X.X., Y.Y. and Z.Z.; formal analysis, X.X.; investigation, X.X.; resources, X.X.; data curation, X.X.; writing—original draft preparation, X.X.; writing—review and editing, X.X.; visualization, X.X.; supervision, X.X.; project administration, X.X.; funding acquisition, Y.Y. All authors have read and agreed to the published version of the manuscript.", please turn to the CRediT taxonomy for the term explanation. Authorship must be limited to those who have contributed substantially to the work reported.

Funding: Please add: "This research received no external funding" or "This research was funded by NAME OF FUNDER grant number XXX." and and "The APC was funded by XXX". Check carefully that the details given are accurate and use the standard spelling of funding agency names at https://search.crossref.org/funding, any errors may affect your future funding.

Institutional Review Board Statement: In this section, please add the Institutional Review Board Statement and approval number for studies involving humans or animals. Please note that the Editorial Office might ask you for further information. Please add "The study was conducted according to the guidelines of the Declaration of Helsinki, and approved by the Institutional Review Board (or Ethics Committee) of NAME OF INSTITUTE (protocol code XXX and date of approval)." OR "Ethical review and approval were waived for this study, due to REASON (please provide a detailed justification)." OR "Not applicable" for studies not involving humans or animals. You might also choose to exclude this statement if the study did not involve humans or animals.

Informed Consent Statement: Any research article describing a study involving humans should contain this statement. Please add "Informed consent was obtained from all subjects involved in the study." OR "Patient consent was waived due to REASON (please provide a detailed justification)." OR "Not applicable" for studies not involving humans. You might also choose to exclude this statement if the study did not involve humans. Written informed consent for publication must be obtained from participating patients who can be identified (including by the patients themselves). Please state "Written informed consent has been obtained from the patient(s) to publish this paper" if applicable.

Data Availability Statement: In this section, please provide details regarding where data supporting reported results can be found, including links to publicly archived datasets analyzed or generated during the study. Please refer to suggested Data Availability Statements in section "MDPI Research Data Policies" at https://www.mdpi.com/ethics. You might choose to exclude this statement if the study did not report any data.

Acknowledgments: In this section you can acknowledge any support given which is not covered by the author contribution or funding sections. This may include administrative and technical support, or donations in kind (e.g., materials used for experiments).

Conflicts of Interest: Declare conflicts of interest or state "The authors declare no conflict of interest." Authors must identify and declare any personal circumstances or interest that may be perceived as inappropriately influencing the representation or interpretation of reported research results. Any role of the funders in the design of the study; in the collection, analyses or interpretation of data; in the writing of the manuscript, or in the decision to publish the results must be declared in this section. If there is no role, please state "The funders had no role in the design of the study; in the collection, analyses, or interpretation of data; in the writing of the manuscript, or in the decision to publish the results".

Sample Availability: Samples of the compounds ... are available from the authors.

Abbreviations

The following abbreviations are used in this manuscript:

MDPI	Multidisciplinary Digital Publishing Institute
DOAJ	Directory of open access journals
TLA	Three letter acronym
LD	Linear dichroism

Appendix A

Appendix A.1

The appendix is an optional section that can contain details and data supplemental to the main text—for example, explanations of experimental details that would disrupt the flow of the main text but nonetheless remain crucial to understanding and reproducing the research shown; figures of replicates for experiments of which representative data are shown in the main text can be added here if brief, or as Supplementary Data. Mathematical proofs of results not central to the paper can be added as an appendix.

Table A1. This is a table caption. Tables should be placed in the main text near to the first time they are cited.

Title 1	Title 2	Title 3
Entry 1	Data	Data
Entry 2	Data	Data

All appendix sections must be cited in the main text. In the appendices, Figures, Tables, etc. should be labeled, starting with "A"—e.g., Figure A1, Figure A2, etc.